

# Microwave frequency standard on $^{25}\text{Mg}^+$ ions: expected characteristics and prospects

I.V. Zalivako, I.A. Semerikov, A.S. Borisenko, K.Yu. Khabarova, V.N. Sorokin, N.N. Kolachevsky

**Abstract.** A scheme of the new frequency standard is reported based on a microwave transition between hyperfine components of the ground state in  $^{25}\text{Mg}^+$  ions. It is proposed to capture ions into a linear quadrupole Paul trap and to perform the laser cooling, as well as to prepare the particle ensemble and to implement detection by using a single laser system based on a semiconductor laser. Characteristics of the suggested frequency standard are estimated.

**Keywords:** microwave frequency standard,  $^{25}\text{Mg}^+$  ions.

## 1. Introduction

Compact frequency standards (FS's) are in great demand in many fields of modern applied physics. They are used in positioning systems, global navigation satellite systems (GNSS) (user and space segments), radio astronomy, telecommunication and fast data transfer. To date, compact microwave references on gas cells with a weight of less than 100 g (for example, Microsemi SA.31m atomic clocks [1]) are commercially available, which provide the relative daily instability at a level of a few parts in  $10^{11}$  with a relative inaccuracy of at least  $10^{-9}$ . Their drawbacks are the necessity of using a buffer gas for increasing the coherence time of an atomic state. Collisions of atoms with a buffer gas result in the frequency shifts that are proportional to a gas pressure. The resulting relative frequency shift is determined by the accuracy of temperature control of the cell and by degradation of the latter [2]. In more complicated and accurate devices, the Ramsey method is used. A primary standard 5071A [3] with a weight of 30 kg (Microsemi) provides a relative daily instability of  $3 \times 10^{-14}$  at a relative inaccuracy of  $5 \times 10^{-13}$ .

One more widespread type of FS's is a hydrogen maser. Hydrogen passive masers (Ch1-1007) produced by the company 'Vremya-Ch' provide a daily instability of  $5 \times 10^{-15}$  at a

relative frequency uncertainty of  $10^{-13}$ . Active masers possess better signal characteristics; however, they are less compact as compared to passive devices. Usually, the weight of hydrogen masers is several tens of kilograms. Masers are specific in rare but substantial frequency jumps, which limit their application without additional frequency references. Such jumps may be caused by the mechanical instability of the internal coating of a hydrogen cell, used for increasing the coherence time of the hydrogen atom state.

Presently, FS's based on gas-cell and passive hydrogen masers are used as on-board GNSS time keepers in many countries. In turn, active hydrogen masers are also successfully used in space experiments. For example, the orbiting radio-telescope 'Radioastron' (Lebedev Physical Institute) launched in 2012 has a Russian active maser, which has operated for over five years [4]. The problem of increasing the compactness and reliability of FS's while keeping high characteristics of the latter is still topical. A compact and reliable frequency standard is needed with a daily relative instability of a few parts in  $10^{15}$ . Various methods are suggested for solving the problem; however, there is no generally accepted opinion which one is optimal.

Note that the required characteristics can be obtained by using transportable optical frequency standards, which presently demonstrate frequency reproducibility characteristics at a level of better than  $10^{16}$  [5]. But such systems are rather cumbersome yet and require an accurate adjustment of the laser optical unit used for cooling, capturing, and reading the metrological transition. In addition, for employing the signal of an optical FS it is necessary to convert the optical frequency to the microwave range, which is made by a femtosecond frequency comb (FFC) [6]. The group headed by M. Gubin at the Lebedev Physical Institute develops a compact optical frequency standard based on a He–Ne laser stabilised by the clock transition in methane, which is integrated into the frequency comb scheme for converting the frequency to the microwave range [7].

Of interest is the use of trapped ensembles of ions in microwave FS's. Large ion clouds (up to  $10^6$ ) can be localised in a Paul trap by a radio-frequency field, which may remove restrictions both on the coherence time of the ion state and on the time of interaction with microwave and optical fields without using a buffer gas. As clock transitions, transitions between hyperfine components of the ground state are usually used. Presently, many research groups investigate the possibility of creating a FS on  $^{199}\text{Hg}^+$  (the transition frequency is 40 GHz) [8],  $^{137}\text{Ba}^+$  (8 GHz) [9],  $^9\text{Be}^+$  (0.3 GHz) [10],  $^{171}\text{Yb}^+$  (12.6 GHz) [11] and  $^{113}\text{Cd}^+$  (15.2 GHz) ions [12]. Of particular interest is the microwave standard on  $^{199}\text{Hg}^+$  ions, which demonstrates a short-term instability at a level of

I.V. Zalivako, A.S. Borisenko, K.Yu. Khabarova, N.N. Kolachevsky

P.N. Lebedev Physical Institute, Russian Academy of Sciences, Leninsky prosp. 53, 119991 Moscow, Russia; International Center for Quantum Optics and Quantum Technologies (Russian Quantum Center), ul. Novaya 100, Skolkovo, 143025 Moscow, Russia; Moscow Institute of Physics and Technology (State University), Institutskii per. 9, 141707 Dolgoprudnyi, Moscow region, Russia; e-mail: zalivako.ilya@yandex.ru;

I.A. Semerikov, V.N. Sorokin P.N. Lebedev Physical Institute, Russian Academy of Sciences, Leninsky prosp. 53, 119991 Moscow, Russia; International Center for Quantum Optics and Quantum Technologies (Russian Quantum Center), ul. Novaya 100, Skolkovo, 143025 Moscow, Russia; e-mail: ilia179@mail.ru

Received 9 March 2017; revision received 25 March 2017  
Kvantovaya Elektronika 47 (5) 426–430 (2017)  
Translated by N.A. Raspopov

$5 \times 10^{-14} \tau^{-1/2}$ , and on  $^{113}\text{Cd}^+$  ions with a short-term instability of  $6 \times 10^{-13} \tau^{-1/2}$ .

In the present work, we consider the possibility of employing the  $^{25}\text{Mg}^+$  ion for developing a microwave frequency reference. Despite the relatively small splitting of hyperfine components of the ground state (1.8 GHz), the magnesium ion possesses certain advantages. In particular, its level structure allows cooling, preparing, and interrogation of the ensemble by means of a single laser system and several optical modulators. We have demonstrated the trapping and laser cooling of magnesium ions in [13]; after a minor further modification, the setup will enable us to study characteristics of the hyperfine transition of the ground state of the magnesium ion.

## 2. Energy level diagram of $^{25}\text{Mg}^+$ and suggested experimental scheme

The diagram of energy levels of the  $^{25}\text{Mg}^+$  ion (the nuclear spin,  $I = 5/2$ ) intended for use in the frequency reference is shown in Fig. 1. For the clock transition we suggest the magneto-dipole transition between components of the hyperfine structure of the ground state with the frequency  $\nu_{\text{HFS}} = 1.789$  GHz. A contribution of the linear Doppler effect will be suppressed due to the Lamb–Dicke effect, because ions will be localised in a volume *a fortiori* smaller than the wavelength. However, for suppressing the quadratic Doppler effect and convenient readout of the transition it is necessary to realise laser cooling.

The Doppler cooling of  $^{25}\text{Mg}^+$  ions is realised on the transition between the levels  $^2\text{S}_{1/2}$  and  $^2\text{P}_{3/2}$ , which is also used for quantum state preparation and detection. The  $^2\text{S}_{1/2} \rightarrow ^2\text{P}_{3/2}$  transition at a wavelength of 280 nm has a natural linewidth,  $\Gamma = 2\pi \times 41.4$  MHz, and the saturation intensity,  $I_{\text{sat}} = 250$  mW cm $^{-2}$ . Although the transition is almost cyclic, ions may be lost from the cooling cycle. The hyperfine structure of

the upper level with the splitting on the order of  $\Gamma$  leads to the nonresonance excitation of the  $^2\text{S}_{1/2}(F=3, m_F=3) \rightarrow ^2\text{P}_{3/2}(F=3, m_F=3)$  transition. In the result, part of ions are in the long-lived state  $^2\text{S}_{1/2}(F=2)$  and are lost from the cooling process. To return ions to the cooling cycle, repumping radiation is needed, which couples the levels  $^2\text{S}_{1/2}(F=2)$  and  $^2\text{P}_{3/2}(F=3)$ .

The scheme suggested for the experiment is shown in Fig. 2. Magnesium atoms are held in the linear quadrupole Paul trap, which was thoroughly described in [13]. Secular frequencies of  $^{25}\text{Mg}^+$  ion motion in the trap in the radial and axial directions are  $\omega_{\text{rad}} \approx 2\pi \times 500$  kHz and  $\omega_{\text{ax}} \approx 2\pi \times 100$  kHz, respectively; the trap depth is  $D \approx 3$  eV. Ions are loaded by the method of impact ionisation of magnesium atoms by an electron beam directly in a trap volume. Since the magnesium atomic beam has a natural isotope composition and the ionisation method is not selective, the fraction of  $^{25}\text{Mg}^+$  ions among other isotopes is 10%. The presence of other isotopes in the trap is not desirable because this would result in particle heating and signal-to-noise ratio worsening. Hence, after loading into the trap, ions of other species should be removed. This can be done by varying the amplitude of the alternating potential across the trap electrodes and adding a constant potential, which will shift the trap parameters to the domain where the motion of only the  $^{25}\text{Mg}^+$  ion will be stable. For realising the frequency reference, we plan to trap about  $10^6$   $^{25}\text{Mg}^+$  ions.

An important advantage of ion frequency standards is a long lifetime of ions in a trap, which ensures a long time of interaction between the exciting radiation and particles. The ion lifetime in the trap is mainly limited by the two factors: by the particle radiofrequency heating, which is related to the ion–ion interaction and deviations of the trapping potential from the quadrupole, and by collisions of trapped ions with neutral atoms [13–15]. Such collisions may lead to a charge exchange between the ion and the neutral atom; hence, the

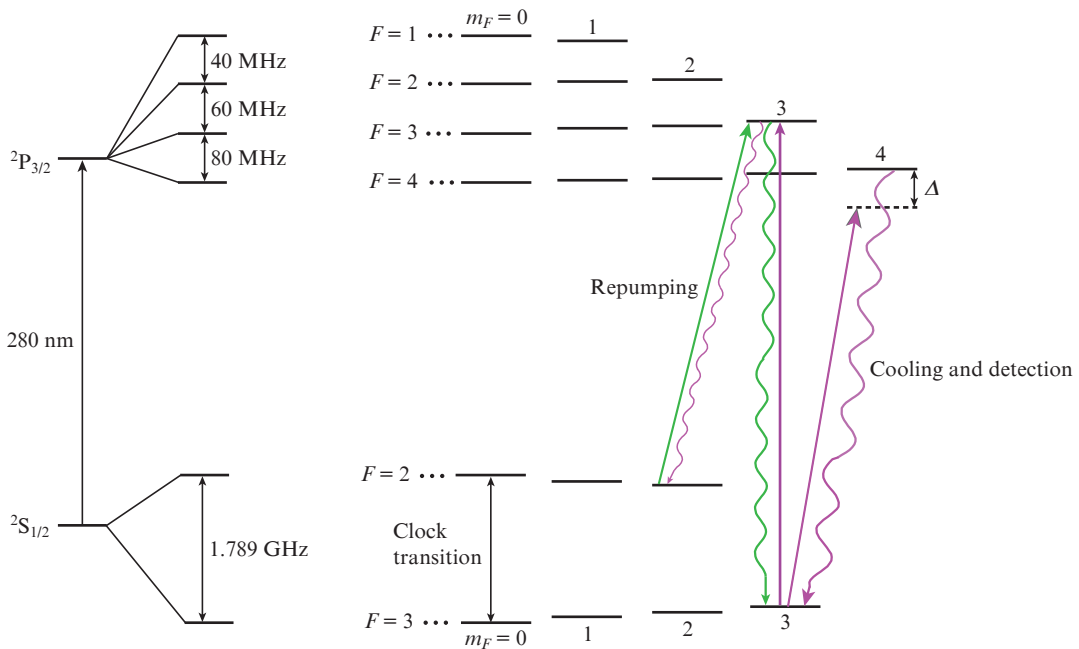


**Figure 1.** Energy level diagram of the  $^{25}\text{Mg}^+$  ion used in the experiment. The radiation of a cooling laser is red detuned from resonance by the value  $\Delta \approx \Gamma/2$ . The repumping radiation is used for returning the ions, nonresonantly excited by the cooling radiation to the  $^2\text{S}_{1/2}(F=2)$  state, into the cooling cycle.

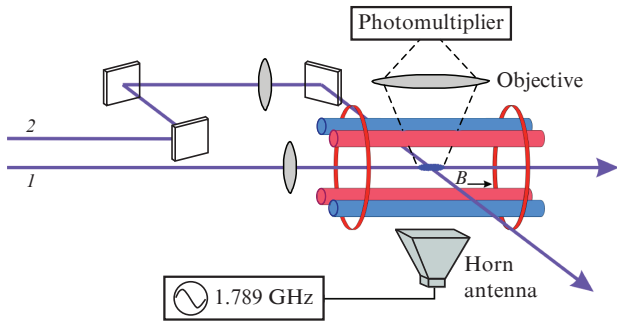


**Figure 2.** Schematic of the setup for spectroscopy of the clock transition in  $^{25}\text{Mg}^+$  ions: (1, 2) laser beams (280 nm), which provide the Doppler cooling, preparation of the quantum state, and detection of the fraction of excited ions; the clock transition is excited by a pyramidal horn antenna; the ion fluorescence is detected by a wide-aperture objective and photomultiplier;  $B$  is the magnetic field for splitting the levels over magnetic quantum numbers.

ion may be lost from the trap. In order to suppress the second factor, the trap is placed inside a vacuum chamber, in which the pressure is maintained at a level of  $2 \times 10^{-10}$  mbar by means of an ion getter pump, which provides the ion lifetime in the trap on the order of dozens of minutes.

Without a magnetic field, ions may transfer between energy-degenerated magnetic components due to collisions with other ions. This substantially reduces the coherence time of a particle quantum state and, correspondingly, the signal/noise ratio of the designed frequency standard. A magnetic field with an induction  $B \approx 10$  mGs applied in the direction

along the trap axis will split the magnetic sublevels and prevent transitions between magnetic components. The exact value of the magnetic field providing the optimal signal/noise ratio should be determined experimentally.

It is assumed to use an SRS DS345 oscillator (capable of stabilising its frequency by the signal from a passive hydrogen maser) as a source of microwave radiation. To amplify the signal, we have developed a pyramidal horn antenna with a linear waveguide having dimensions  $54 \times 107 \times 154$  mm, which delivers the signal to the ion trap volume. For selective excitation of  $\pi$ -transitions between hyperfine components of the ground state it is important that the polarisation direction of the magnetic induction vector be parallel to the trap axis.

The Doppler cooling, optical pumping and detection of magnesium ions are provided by the laser system described in [16]. An optical scheme suggested for the experiment is presented in Fig. 3. The radiation at 280 nm is divided by a polarisation beam splitter into two parts. The beams obtained are detuned in frequency by acousto-optical modulators (AOMs) in the two-pass configuration in such a way that the frequency difference between the beams corresponded to that of the hyperfine splitting of the ground state  $\nu_{\text{HFS}}$ . Thus, the radiation of one of the beams is in resonance with the  $^2\text{S}_{1/2}(F=3) \rightarrow ^2\text{P}_{3/2}$  transition and the radiation of the second beam is in resonance with the  $^2\text{S}_{1/2}(F=2) \rightarrow ^2\text{P}_{3/2}$  transition. In addition, the AOMs allow one to switch on and off the beams quickly and independently. In experiments, beam polarisation can be changed by electro-optical modulators (EOMs) or half-wave phase plates placed on motorised translation stages. Fluorescence of  $^{25}\text{Mg}^+$  ions can be detected by using a photomultiplier. The radiation from ions will be collected by using a wide-aperture objective.

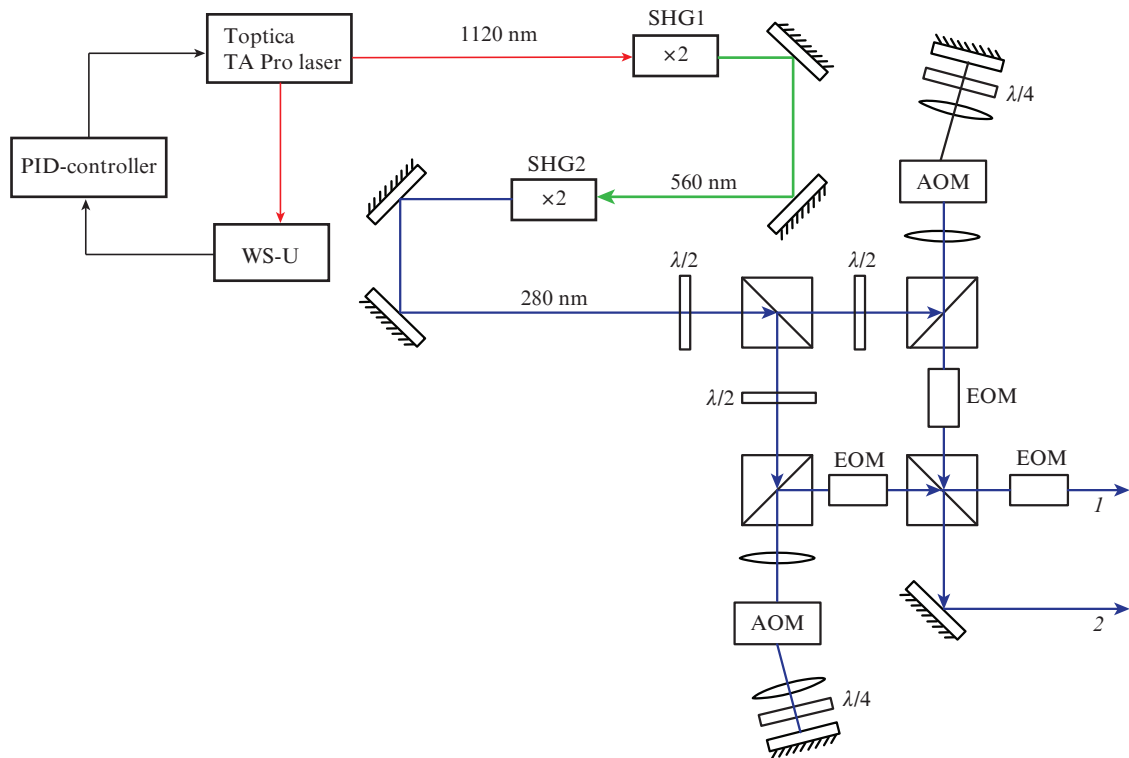


**Figure 3.** Optical scheme of forming the radiation for laser cooling, pumping, and detection of the fraction of excited ions  $^{25}\text{Mg}^+$ : SHG1 and SHG2 are optical frequency doublers on nonlinear LBO and BBO crystals, respectively; (1, 2) laser beams introduced to the ion trap (Fig. 2); WS-U is highly-stable wavelength meter used for stabilising the operation wavelength of a Toptica TA Pro laser.

### 3. Spectroscopy of the clock transition

After ions have been loaded into the trap and selected with respect to their atomic mass, a cyclic process of probing the clock transition starts. A measuring cycle for the clock transition comprises four stages. They are the Doppler cooling of ions, the optical pumping, the excitation of the clock transition by the Ramsey scheme, and the detection of the fraction of excited ions.

For the cooling,  $\sigma^+$ -polarised cooling and repumping beams are switched on for a time period  $t_{\text{cool}} \approx 1$  s. The first beam is red detuned by  $I/2$  from the  $^2\text{S}_{1/2}(F=3) \rightarrow ^2\text{P}_{3/2}(F=4)$  transition. The repumping beam, which resonantly couples the levels  $^2\text{S}_{1/2}(F=2) \rightarrow ^2\text{P}_{3/2}(F=3)$ , is needed for returning into the cooling cycle the ions, which have transferred to the state  $^2\text{S}_{1/2}(F=2)$  due to nonresonance excitation of the  $^2\text{S}_{1/2}(F=3) \rightarrow ^2\text{P}_{3/2}(F=3)$  transition by the cooling laser.

As the clock transition, we suggest using the  $^2\text{S}_{1/2}(F=2, m_F=0) \rightarrow ^2\text{S}_{1/2}(F=3, m_F=0)$  transition. The frequency  $\nu_0$  of the transition between the magnetic components having zero values of the momentum projection onto the trap axis depends on the magnetic field only in the second order with respect to the field, whereas the frequencies of transitions between other magnetic components depend on the field intensity in the first order. The frequency of the clock transition depends on the value of the magnetic field:  $\nu_0(B) = \nu_{\text{HFS}} + \eta B^2$ , where  $\nu_{\text{HFS}}$  is the transition frequency with an absent magnetic field and the coefficient  $\eta = 2.199$  kHz  $\text{Gs}^{-2}$ . Pumping to the level  $^2\text{S}_{1/2}(F=2, m_F=0)$  can be realised by using two laser beams. One beam should be in resonance with the  $^2\text{S}_{1/2}(F=2) \rightarrow ^2\text{P}_{3/2}(F=2)$  transition, have a linear polarisation directed along the trap axis. The second beam should couple the levels  $^2\text{S}_{1/2}(F=3)$  and  $^2\text{P}_{3/2}(F=3)$ . To provide a high pumping efficiency, the polarisation and direction of this beam should periodically change in order to alternatively excite the  $\pi$ - and  $\sigma^+$ -transitions.

To compensate for the frequency shift of the clock transition due to the quadratic Zeeman effect, it is necessary to measure the magnetic field in the ion trap volume with a high precision. Conventionally, such a measurement is performed in the experimental cycle by measuring the frequency difference between the  $^2\text{S}_{1/2}(F=2, m_F=\pm 2) \rightarrow ^2\text{S}_{1/2}(F=3, m_F=\pm 2)$  transitions. Since the frequencies of these transitions,  $\nu_2$  and  $\nu_{-2}$ , linearly depend on the magnetic field, the induction of the latter can be calculated by the formula  $B = \kappa(\nu_{-2} - \nu_2)$ , where  $\kappa = 0.267$  Gs  $\text{MHz}^{-1}$ . In deriving the formula, we used the coefficients  $g_J = 2.002254(3)$  [17] and  $g_I = 3.419804(27)$  [18] for the electron and nuclear g-factors, respectively. Pumping to levels  $^2\text{S}_{1/2}(F=2, m_F=\pm 2)$  can be performed similarly to pumping to the level with  $m_F=0$  except for that the first beam should be, respectively,  $\sigma^+$ - or  $\sigma^-$ -polarised (Fig. 4).

After the pumping to the required magnetic sublevel, the clock transition can be excited by two radiofrequency  $\pi/2$ -pulses. Durations of the pulses and the time interval between them will be optimised experimentally for obtaining the best stability and accuracy. After excitation of the clock transition, the fraction of excited ions will be determined using a photomultiplier by the level of fluorescence in scattering the cooling laser radiation.

### 4. Estimate of the main characteristics

The main effects leading to a frequency shift of the clock transition in microwave frequency standards are the second-order

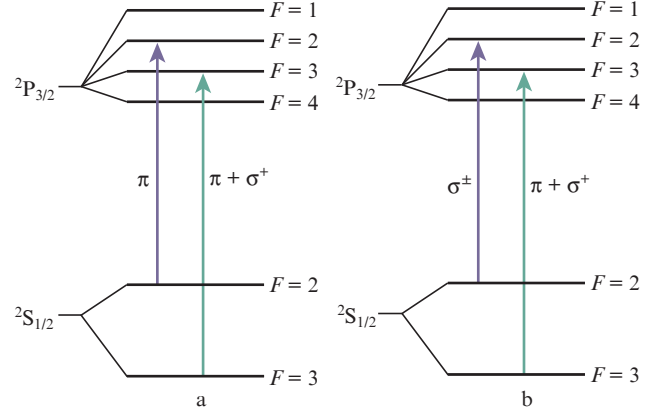


**Figure 4.** Schematic for optical pumping of the  $^{25}\text{Mg}^+$  ion to sublevels (a)  $^2\text{S}_{1/2}(F=2, m_F=0)$  and (b)  $^2\text{S}_{1/2}(F=2, m_F=\pm 2)$ .

Doppler effect and quadratic Zeeman effect. Contributions from other effects, such as the dynamic Stark effect caused by the fields of the trap and by equilibrium thermal emission, as well as the collision shift, affect the frequency and accuracy of the clock transition substantially weaker.

Since the area of ion localisation in the trap is noticeably smaller than the half-wavelength of the clock transition radiation, the first-order Doppler effect is suppressed, and only the second-order Doppler effect contributes into the shift. The corresponding relative frequency shift can be estimated by the formula [19]:

$$\frac{\delta\nu_{\text{D}}}{\nu} = -\frac{3k_{\text{B}}T}{2mc^2} \left(1 + \frac{2}{3}N_{\text{D}}^k\right),$$

where  $k_{\text{B}}$  is the Boltzmann constant,  $T$  is the temperature of the ion cloud,  $m$  is the ion mass, and  $c$  is the speed of light. The summand  $N_{\text{D}}^k$  characterises the Doppler shift related to the micromotion of the ion and for similar trap configurations with laser cooling it is conventionally  $\sim 3$ . At the temperature uncertainty of 1 K, for the  $^{25}\text{Mg}^+$  ion the relative frequency uncertainty  $\delta\nu_{\text{D}}/\nu$  related to the Doppler effect will be approximately  $2 \times 10^{-14}$ .

The uncertainty due to the quadratic Zeeman effect can be estimated as

$$\frac{\delta\nu_{\text{Z}}}{\nu} = \frac{2\eta B \delta B}{\nu_{\text{HFS}}}.$$

At  $\delta B \approx 1$   $\mu\text{mH}$ , the uncertainty is  $\delta\nu_{\text{Z}}/\nu = 3 \times 10^{-14}$ .

The theoretically achievable short-term relative frequency instability of the future standard can be estimated by the known formula [20]

$$\sigma_y(\tau) = \frac{1}{2\pi\nu_{\text{HFS}}\Delta t_{\text{R}}\text{SNR}} \sqrt{\frac{T_{\text{c}}}{\tau}}, \quad \tau \geq T_{\text{c}} \geq 2\Delta t_{\text{R}},$$

where  $\Delta t_{\text{R}}$  is the time interval between successive microwave pulses in the Ramsey scheme, SNR is the signal-to-noise ratio,  $T_{\text{c}}$  is the duration of the frequency measurement cycle, and  $\tau$  is the signal averaging time. If the quantum projection noise is the only source of noise in the measurement process, then  $\text{SNR} = \sqrt{N_{\text{i}}}$ , where  $N_{\text{i}}$  is the number of ions in trap. At  $\nu_{\text{HFS}} = 1.789$  GHz,  $\Delta t_{\text{R}} = 1$  s,  $T_{\text{c}} = 2\Delta t_{\text{R}}$  and  $N_{\text{i}} = 10^6$ , the short-term relative frequency instability for this standard can

be estimated as  $1.3 \times 10^{-13} \tau^{-1/2}$ . However, there are other sources of noise, which worsen the signal-to-noise ratio and, hence, affect the stability of the standard.

The standard suggested is predicted to exhibit worse relative instability than a microwave standard on mercury ions. The main reason for that is a smaller hyperfine splitting of the ground state. However, our experiments with a compact trap and original optical scheme give a chance to lay the scientific and technological groundwork for new-generation microwave ion standards with laser cooling.

Thus, we have considered the microwave frequency standard on the hyperfine splitting of the ground state of the  $^{25}\text{Mg}^+$  ion, elaborated the experimental scheme, and established the interrogation sequence for the clock transition. A frequency uncertainty of the standard was estimated as  $\delta\nu/\nu \approx 3.6 \times 10^{-14}$  at moderate requirements to fluctuations of the magnetic field and cloud temperature. The estimate of the short-term relative instability of the standard is  $\sigma_y(\tau) = 1.3 \times 10^{-13} \tau^{-1/2}$ . In addition to applied aspects, the measurements suggested will more exactly specify the constant of the hyperfine splitting for magnesium.

**Acknowledgements.** The work was supported by the Russian Science Foundation (Grant No. 16-12-00096).

## References

1. <https://www.microsemi.com/products/timing-synchronization-systems/embeddedtiming-solutions/components/sa-31m-sa-33m-amp-sa-35m#documents>.
2. Bandi Th., Affolderbach Ch., Stefanucci C., Merli F., Skrivervik A.K., Mileti G. *IEEE Transac. Ultrason., Ferroelectr., and Frequency Control.*, **61**, 1769 (2014).
3. [https://www.microsemi.com/document-portal/doc\\_view/133269-5071a](https://www.microsemi.com/document-portal/doc_view/133269-5071a).
4. Utkin A., Belyaev A., Pavlenko Yu. *Abst. VI Int. Symp. 'Metrology of Time and Space'* (Mendeleevo, 2012) pp 85–87.
5. Riehle F. *Nature Photon.*, **11**, 25 (2017).
6. Wilken T., Lezius M., Hänsch T.W., Kohfeldt A., Wicht A., Schkolnik V., Krutzik M., Duncker H., Hellmig O., Windpassinger P., Sengstock K., Peters A., Holzwarth R. *Proc. CLEO: Applications and Technol.*, AF2H.5 (2013).
7. Kireev A.N., Tausenev A.V., Tyurikov D.A., Shelkovnikov A.S., Shepelev D.V., Konyashchenko A.V., Gubin M.A. *Quantum Electron.*, **46**, 1139 (2016) [*Kvantovaya Elektron.*, **46**, 1139 (2016)].
8. Burt E.A., Diener W.A., Tjoelker R.L. *IEEE Transac. Ultrason., Ferroelectr., and Frequency Control.*, **55** (12), 2586 (2008).
9. Knab H., Niebing K., Werth G. *IEEE Trans. Instr. Measurement*, **34** (2), 242 (1985).
10. Bollinger J.J., Heinzen D.J., Itano W.M., Gilbert S.L., Wineland D.J. *IEEE Trans. Instr. Measurement*, **40** (2), 126 (1991).
11. Park S.J., Manson P.J., Wouters M.J., Warrington R.B., Lawn M.A., Fisk P.T.H. *Frequency Control Symposium, 2007 Joint with the 21st European Frequency and Time Forum. IEEE International*, 613 (2007).
12. Miao K., Zhang J.W., Sun X.L., Wang S.G., Zhang A.M., Liang K., Wang L.J. *Opt. Lett.*, **40** (18), 4249 (2015).
13. Semerikov I.A., Zalivako I.V., Shpakovskii T.V., Borisenko A.S., Khabarova K.Yu., Sorokin V.N. *Quantum Electron.*, **46**, 935 (2016) [*Kvantovaya Elektron.*, **46**, 935 (2016)].
14. Harmon T.J., Moazzan-Ahmadi N., Thompson R.I. *Phys. Rev. A*, **67**, 013415 (2003).
15. Rapp D., Francis W.E. *J. Chem. Phys.*, **37**, 2631 (1962).
16. Shpakovsky T.V., Zalivako I.V., Semerikov I.A., Golovizin A.A., Borisenko A.S., Khabarova K.Yu., Sorokin V.N., Kolachevsky N.N. *J. Russ. Laser Res.*, **37**, 440 (2016).
17. Bollinger J.J. *Bull. Am. Phys. Soc.*, **37**, 1117 (1992).
18. Itano W.M., Wineland D.J. *Phys. Rev. A*, **24**, 1364 (1981).
19. Prestage J.D., Tjoelker R.L., Maleki L. *Joint Meeting EFTF - IEEE IFCS*, **124** (1), 121 (1999).
20. Fisk P.T.H. *Rep. Progr. Phys.*, **60**, 761 (1997).